Author Manuscript
Accepted for publication in a peer-reviewed journal

NIST National Institute of Standards and Technology • U.S. Department of Commerce

Published in final edited form as:
J Vac Sci Technol B Nanotechnol Microelectron. 2016 ; 34(3): . doi:10.1116/1.4942612.

Uranium Ion Yields from Monodisperse Uranium Oxide Particles

Nicholas Sharp[a],
National Institute of Standards and Technology, 100 Bureau Dr, Mail Stop 8371, Gaithersburg, Maryland 20899

John D. Fassett, and
Dakota Consulting, Inc., 1110 Bonifant Street, Silver Spring, Maryland 20910

David S. Simons[b]
National Institute of Standards and Technology, 100 Bureau Dr, Mail Stop 8371, Gaithersburg, Maryland 20899

Secondary ion mass spectrometry (SIMS) plays an important role in nuclear forensics through its ability to identify isotopic ratios of particles accurately and precisely from samples obtained by inspectors [1]. As the particle mass can be on the order of subpicograms, it is important to maximize the sample utilization efficiency of U^+ to make high-quality isotopic measurements. The influence of primary ion beam species and polarity on U^+ sample utilization efficiency has been previously investigated by Ranebo *et al.* [2]. However, the effect of sample substrate on uranium ion production efficiency and sputtering profile has not been investigated. This work will explore those influences on sample utilization efficiency by analyzing mono-disperse uranium oxide microspheres deposited onto graphite and silicon planchets. The particles were mapped using an automated scanning electron microscope and their coordinates were converted to the SIMS coordinate system using fiducial marks. Results indicate higher U^+ sample utilization efficiencies when sputtering with O^- and O_2^- on graphite planchets compared with O_2^+, whereas O_2^- gave higher U^+ sample utilization efficiencies with silicon wafers compared to O^- and O_2^+. Additionally, during sputtering of uranium particles on silicon wafers with O^- and O^{2-}, a sudden drop in U^+ signal intensity was observed which was not present during sputtering with O_2^+ or any primary ion species for particles on graphite. This drop in U^+ signal intensity occurred simultaneously with an increase in UO^+ and UO_2^+ signals, indicating a change in the local matrix around the uranium particle that is unique to silicon compared to graphite.

I. INTRODUCTION

The measurement of particulate matter obtained from nuclear monitoring agents is important in assessing whether international declarations are properly followed at nuclear facilities [3, 4]. Particles can provide insight into the uranium enrichment processes being conducted at a facility as well as the provenance of the source material [2-8]. Analyzing these particles can

[a]Electronic nicholas.sharp@nist.gov.
[b]American Vacuum Society member.

be difficult due to their small (<1 μm) size and subsequent low mass of analyte present. Secondary ion mass spectrometers (SIMS) are capable of measuring micrometer-sized particles with masses on the order of picograms and providing isotopic ratios with relative uncertainties on the order of less than 1 % for major isotopes [8-10]. Samples are analyzed by using a primary ion beam to sputter the sample material, ejecting charged and uncharged elemental and molecular species. The secondary ions are subsequently accelerated into the mass spectrometer, separated by mass and energy, and detected using an electron multiplier or Faraday cup. The fraction of detected secondary ions of a species compared to the total number of sample atoms of that species that are sputtered from a sample is known as the sample utilization efficiency, or useful yield, and it incorporates the sputtering yield, transmission, and detection efficiencies. Sample utilization efficiencies vary depending on analyte matrix and morphology with uranium (U^+) yields of 0.7 % when in glass with a CAMECA IMS-3F instrument [11], 2.9 % for clay particles loaded with uranium using an IMS-4F [12], and 0.27 to 1.2 % for uranium oxide particles using both an IMS-6F and IMS-1270 [2, 13].

As the mass of a typical particle is small, it is important to understand what variables have an effect on the sample utilization efficiency in order to select appropriate measurement parameters to maximize instrument sensitivity, such as primary ion beam species and sample substrate. Determining the influence of the analytical measurement parameters requires that the mass of the analyte particles be precisely and accurately known. Monodisperse uranium particles produced from CRM U020-A (a uranium isotopic standard distributed by New Brunswick Laboratory [14]) material meets both requirements [2, 15]. Recently, differences in sample utilization efficiencies for U^+ ions using different primary ion beams have been observed [2]. However, the effect of sample substrate on uranium ion efficiency and sputtering profile has not been investigated. In this work we measure the effect of the sample substrate on sample utilization efficiency by analyzing identically prepared monodispersed particles produced from U020-A with various primary ion beams on a silicon wafer and a graphite planchet.

II. EXPERIMENTAL

Uranium oxide microspheres were produced at the Institute for Transuranium Elements (ITU) from CRM U020-A using an aerosol generation system that creates highly uniform droplet sizes from the dissolved uranium standard [15]. The droplets then were heated in a coupled furnace to dry the uranyl nitrate aerosol droplets, generating particles with reported masses of 2.58 pg (± 0.17 pg 1σ). [2, 15]. A dispersion of particles on a carbon substrate was prepared at ITU by placing the filter with captured calcined uranium microspheres into an isopropanol solution and ultra-sonicating it to suspend the particles. An aliquot of the solution was deposited and dried on a polished pyrolytic graphite SIMS planchet that was then gold-coated and sent to the National Institute of Standards and Technology (NIST). The sample on a p-type <100> silicon substrate was prepared at NIST using particles from the same batch as the carbon sample, but at a lower spatial density.

A. Particle mapping

Particle locations on the planchets were identified using automated scanning electron microscopy/energy-dispersive x-ray spectroscopy (SEM/EDX) particle imaging and analysis instrumentation. These measurements were made on a Tescan MIRA instrument with a PulseTorr silicon drift detector. Reading and processing the data was done with internally produced NIST Graf software. Analysis of a small portion of the graphite planchet revealed that the planchet was densely populated with particles. A total of 8736 particles were identified in two sub-areas that were scanned, corresponding to a total area of approximately one-third of the droplet region on the planchet. The mapping was halted at this point due to the overabundance of particles already identified. The silicon wafer was not as densely populated as the carbon planchet, resulting in the location mapping of 644 particles over the entire deposit area. Figure 1 shows the particle distribution determined by SEM/EDX for the silicon planchet. The carbon planchet is similar in appearance although with many more particles present.

Three fiducial marks were scribed on the carbon and silicon substrates prior to the SEM/EDX measurements and their positions were measured in the coordinate system of the SEM. These fiducial marks were used to transform the coordinate system to that of the SIMS system using in-house data analysis software.

The SEM/EDX provides dimensions as well as elemental and position measurements for each particle and supplies a thumbnail image and spectrum for each. The particles were classified as: 1) uranium-rich spheres; 2) uranium-containing particles other than spheres; and, 3) all others. Spheres were defined as having an aspect ratio (largest/smallest chord) of less than 1.3. The number distribution of these classified particles identified on the carbon planchet was 1367, 6186, and 1183 particles, respectively, out of a total of 8736 particles. The entire silicon wafer contained 398 uranium spheres, 1 other uranium containing particle, and 245 other particles. During the particle formation process multiple droplets could merge to form larger particles which are distinguishable from single mass particles based on their average diameter. To ensure that only single droplet particles were analyzed, any particles with an average diameter larger than 1.2 μm were rejected for analysis.

The positions of uranium-rich spheres in the mapped region of the carbon planchet and on the entire silicon wafer were plotted and ones that were reasonably isolated from neighboring particles were chosen for analysis. The specifications for particle proximity varied between the samples due to the particle density. The silicon wafer contained 202 spheres that were separated by more than 100 μm from their nearest neighbor, enabling the use of a Köhler illumination beam with nominal beam diameter of 50 μm. However, the particles on the carbon planchet were spaced such that a focused beam with a small raster was more suitable for particle analysis. Therefore, separations on the order of 50 μm or more were sufficient for particle analyses with a 10 μm × 10 μm raster. This procedure ensures that only one particle is sputtered during each analysis and that no residual material is deposited on neighboring particles which may affect their analyses.

Before SIMS analysis of a particle, the original SEM/EDX data were checked to verify that the particle dimensions and aspect ratio indicated a spherical particle, and its thumbnail

image was examined to verify that the particle had a circular outline and had no other particles in the field of view. The key data are particle position, average diameter, aspect ratio, and elemental signature. Only particles which met the predefined criteria for a candidate particle were selected for analysis.

B. SIMS measurements

The SIMS analyses were conducted with a CAMECA IMS-1270 E7 which is a magnetic sector, double-focusing mass spectrometer. It is capable of both imaging a sample as well as performing isotopic analyses with mass resolutions ranging from 2 000 to 25, 000. The IMS-1270 E7 is particularly suited for uranium isotopic analyses as the mass resolving power can be set to reject all molecular isobaric interferences, with the exception of uranium hydrides, and it can achieve levels of precision for isotopic measurements of uranium in particles that are compatible with the requirements of nuclear safeguards [1].

To compare the total ion efficiencies for different primary ion beams, the microspheres were sputtered under identical secondary optic settings with only the primary ion beam species, polarity, and sample substrate varying. For all analyses the $^{238}U^{+}$ signal was measured versus time in the depth profiling mode of signal acquisition. For the silicon wafer, the primary beam was in Köhler illumination mode with a slightly elliptical 50 μm diameter beam shape and a secondary ion acceptance window of 50 μm × 50 μm. Due to the previously mentioned higher density of particles on the carbon planchet, a 50 μm diameter beam would have severely restricted the number of candidate uranium particles available for analysis. Instead, a focused ion beam, with a diameter smaller than 10um but otherwise unmeasured, was used with a 10 μm × 10 μm raster combined with dynamic transfer optics during the analysis. Some particles were able to be analyzed using Köhler illumination and their results agreed with the 10 μm × 10 μm rastered particles. As the particles were too small to visualize using the optical microscope of the SIMS instrument, they were located by moving the sample stage to their calculated locations in the SIMS coordinate system and were visualized by secondary ion imaging using a low intensity (10x reduced) primary beam to identify and center the particle while minimizing sample sputtering. Locating the particles on Si was additionally impeded by a background coating of uranium on the planchet that was present along the dried droplet rings from the isopropanol deposition, but was not as significant in the inner regions away from the droplet edges. This uranium background sputtered away quickly; however, if a particle was located in a background-rich region it was rejected as a candidate particle due to the potential influence of the background on the measurement. The presence of a background could be due to some of the uranium microspheres dissolving in the isopropanol solution. This background effect was also observed in a previous study [2].

The primary ion current was selected based on the goal of consuming the entire particle within 600 s to 1000 s and was approximately 15 nA for Köhler mode and less than 1 nA for a focused beam with a 10 μm × 10 μm raster area. Secondary optic settings were chosen to maximize the transmission efficiency so accurate optimal total ion efficiency could be determined. To this end, the field aperture was set at 8000 μm, defining a field-of-view on

the sample of 50 μm × 50 μm, entrance slit at 250 μm, and exit slit at 500 μm for both silicon and carbon planchets. Primary and secondary settings are summarized in Table I.

III. RESULTS AND DISCUSSION

A. Sample utilization efficiencies

Sample utilization efficiency is defined as the total number of uranium ions detected by the instrument divided by the number of uranium atoms removed by sputtering, i.e., $\Sigma U^+/U_{total}$. This efficiency includes the efficiencies of the ionization process for the measured species, instrumental transmission and ion detection. The absolute measurement of sample utilization efficiency requires a sample with a known amount of uranium atoms. The U020-A microspheres, with 2.58 pg (± 0.17 pg 1σ) per particle and known isotopic composition, serve this purpose. With U020-A having a nominal ^{238}U abundance of 98 % there are 6.4 (± 0.4 1σ) × 10^9 atoms of ^{238}U present in each uranium microsphere. Typical O^-, O_2^-, and O_2^+ profiles for particle sputtering on silicon (a), and graphite (b) are shown in Figure 2. The sputtering process was stopped after the signal had decreased to 10% of the maximum intensity. The unsputtered remainder of the particle would account for small increases to the sample utilization efficiency, which are insignificant compared to the uncertainties of the measurements (i.e., 1.05 % vs 1.02 % at 10 % max signal intensity for O_2^+ on carbon). The integrated uranium signal determined in the depth profile mode, i.e., the areas under the curves in Figure 2, provides the numerator for this calculation. The efficiency results are presented in Table II for the rastered O^-, O_2^-, and O_2^+ primary ion beams on carbon and the Köhler illumination beams on silicon as well as a comparison with previously measured values by Ranebo *et al*, [2].

Sample utilization efficiencies are shown in Table II and analysis by an unequal variance t-test shows that O_2^- gives the highest efficiencies on Si wafers whereas both negative polarity beams give similarly high results in graphite. This is in agreement with other work [2] from uranium particles on polished graphite substrates. However, the higher ion source brightness and better focusing characteristics of O_2^+ relative to O^- may override efficiency differences for certain applications such as automated particle measurements made by scanning ion imaging where image resolution and data acquisition rate are both important. It is important to note that the impact energy and angle of incidence for each of the primary ion beams differ from each other, therefore the differences in efficiency between them should not be attributed solely to the polarity of the primary ion beams. Higher efficiencies were noted with O^- and O_2^- on the graphite substrates while silicon had the higher efficiency with O_2^+.

The shapes of the particle sputter profiles differ between the two substrates. Profiles with a carbon planchet are typically steadily increasing in intensity at the beginning (Figure 2(b)), reach a maximum, and then decay roughly exponentially until the signal has reached 10 % of the maximum at which point the primary ion beam is turned off. Profiles with a silicon wafer (Figure 2(a)) have a similar buildup in intensity near the beginning but then have an abrupt drop in signal when sputtering with O^- or O_2^- primary ion beams. The drop appears to be more abrupt with O^- compared to O_2^-. Afterward, the signal decays exponentially in a similar fashion to profiles of particles on the carbon substrate. As the only differences between O^- and O_2^- analyses are the impact energy per ion (23 keV vs 11.5 keV,

respectively) and angle of primary ion incidence, this difference in profile shape could be due to differences in the penetration depths of the two primary ion species. However, the drop in U^+ signal is likely due to the change in the silicon matrix caused by primary ion implantation.

Analyses of the silicon and silicon oxide ion species during particle sputtering on silicon substrates with O^-, O_2^-, and O_2^+ at 3 nA provide additional information into the sputtering process. When monitoring silicon and its oxides all three secondary ion species have the same overall shape when sputtered with O^- or O_2^- as shown in Figure 3.

The most abundant of the silicon-containing ion species is Si^+ (approximately 98 %) followed by SiO^+ and SiO_2^+ and all species slowly increase in signal during the initial stage of sputtering. The first derivative profiles of Si^+, SiO^+ and SiO_2^+ from O^- and O_2^- bombardment show an abrupt increase in Si^+ at approximately 500 s followed by a stable region through the end of the profile. This transition takes place at a later time compared to the previously described U^+ profiles due to the decrease in current from 15 nA to 3 nA in the latter experiment. Analysis of a uranium particle while monitoring the Si^+, U^+, UO^+, and UO_2^+ signals shows that the abrupt increase in Si^+ coincides with the abrupt decrease in U^+ and an increase in UO^+ and UO_2^+ as illustrated in Figure 4. A similar correlation in intensity spikes and drops is observed with O_2^- sputtering, but with less intense spikes spread over a longer time domain.

The relative abundances of uranium oxide species change before, during, and after the abrupt transition. Prior to the transition in U^+ signal at 550 s the relative abundances of the secondary ions is 47:46:7 for U^+:UO^+:UO_2^+. During the transition region (500 s to 617 s) the ratios change to 32:55:13 and immediately after the transition the ratios become 23:57:19 for the remainder of the profile. The key change is a drastic drop in U^+ and a corresponding increase in UO^+ and UO_2^+, leading to the possibility of an increase in oxygen availability in the sputter zone as the cause of the change in abundances of the secondary ions during the sputtering process.

To test the role of oxygen on the profile of uranium particles sputtered on silicon planchets, particles of uraninite were deposited onto a silicon planchet in a similar fashion to the uranium microspheres. An O_2 gas leak was directed at the sample to observe how the profile of the particle was affected by increasing pressures of O_2. Results of that experiment are shown in Figure 5.

The drop in U^+ intensity is clearly present at the base pressure (1×10^{-8} Pa) shown in Figure 5. When increasing the O_2 leak rate to produce a pressure of 1×10^{-5} Pa in the sample chamber the intensity of the signal is reduced overall by a factor of 10 but the drop during the sputtering profile is still present and occurs at the same time as the previous measurement. When the O_2 leak rate was increased to produce a pressure of 1×10^{-4} Pa, the drop was absent from the sputtering profile.

The abrupt drop in these U^+ profiles are similar to what is observed in profiles of boron [16] and copper [17] ions implanted in Si while bombarded with O_2^+ primary ion beams at near normal incidence. In both of these situations it was determined that the Si matrix was

undergoing oxidation near the surface into SiO_x (with x ≤2) [16, 18]. The lack of a drop in U^+ signal intensity when sputtering with O_2^+ compared to O^-/O_2^- primary ion beams in our samples can be explained by the difference in primary ion beam angles between the O^-/O_2^- and O_2^+ ion beams. The negative polarity beams strike the sample at 22.1° from normal whereas the O_2^+ ion beam is at 43.2° from normal. Previous studies have shown a marked decrease in SiOx production depending on primary ion beam angle [16, 19-21]. The addition of oxygen gas likely increases the degree of oxidation of the surface Si [18], resulting in the silicon remaining at an effectively constant oxidation state throughout the sputtering process evidenced by the lack of a drop in the U^+ signal during sputtering at 1×10^{-4} Pa.

IV. SUMMARY AND CONCLUSIONS

The effect of sample substrate on the sample utilization efficiency of uranium particles has been studied with multiple primary ion beams. Overall, graphite has higher sample utilization efficiencies when using O^- and O_2^- compared to silicon while silicon has a higher efficiency when using O_2^+, though still less than O^- and O_2^- when sputtering from graphite. An abrupt drop in U^+ signal occurring at the same moment as an increase in UO^+ and UO_2^+ in the silicon substrate with negative polarity ion beams is indicative of a transition from Si at the surface to SiO_x due to oxidation from primary ion beam implementation. The effect is not observed with O_2^+ due to the larger incidence angle resulting in a decrease in the oxygen loading of the substrate.

ACKNOWLEDGMENTS

We would like to thank Ylva Ranebo for providing the microspheres on a carbon planchet and the particles used to prepare the silicon sample. Also thanks to Abigail Lindstrom for preparing the silicon sample and Nicholas Ritchie for the SEM analyses.

Certain commercial equipment, instruments, or materials are identified in this paper in order to specify the experimental procedure adequately. Such identification is not intended to imply recommendation or endorsement by the National Institute of Standards and Technology, nor is it intended to imply that the materials or equipment identified are necessarily the best available for the purpose.

References

1. Boulyga S, Konegger-Kappel S, Richter S, Sangély L. J. Anal. At. Spectrom. 2015; 30:1469.
2. Ranebo Y, Hedberg PML, Whitehouse MJ, Ingeneri K, Littmann SJ. J. Anal. At. Spectrom. 2009; 24:277.
3. Donohue DL. Anal. Chem. 2002; 74:28A.
4. Kuhn E, Fischer D, Ryjinksi M. Environmental sampling for IAEA Safeguards: A five year review. IAEA Report IAEA-SM-367/10/01. 2001
5. Sturm M. ESARDA Bulletin. 2010; 43:56.
6. Tamborini G, Phinney D, Bildstein O, Betti M. Anal. Chem. 2002; 74:6098. [PubMed: 12498207]
7. Tamborini G. Microchim. Acta. 2004; 145:237.
8. Tamborini G, Betti M, Forcina V, Hiernaut T, Giovannone B, Koch L. Spectromchim. Acta B. 1998; 53:1289.
9. Ranebo Y, Niagolova N, Erdmann N, Eriksson M, Tamborini G, Betti M. Anal. Chem. 2010; 82:4055. [PubMed: 20415437]
10. Wallenius M, Tamborini G, Koch L. Radiochim. Acta. 2001; 89:55.
11. Hervig RL, Mazdab FK, Williams P, Guan Y, Huss GR, Leshin LA. Chem. Geol. 2006; 227:83.

12. Stoffel(s) JJ, Briant JK, Simons DS. J. Am. Soc. Mass Spectr. 1994; 5:852.
13. Hedberg PML, Ingeneri K, Watanabe M, Kuno Y. Isotopic measurements of U particles by Secondary Ionization Mass Spectrometry. Proceedings of the 46th Institute of Nuclear Materials Management (INMM) Annual Meeting. 2005
14. New Brunswick Laboratory. [11/4/2015] Certificate of Analysis CRM U020-A. http://science.energy.gov/~/media/nbl/pdf/price-lists/certificates/CRM_U020-A_10_Milligram_Sample_Size_March_2008.pdf
15. Erdmann N, Betti M, Stetzer O, Tamborini G, Kratz JV, Trautmann N, van Geel J. Spectromchim. Acta B. 2000; 55:1565.
16. Wittmaack K. Surf. Interface Anal. 1996; 24:389.
17. Boudewijn PR, Akerboom HWP, Kempeners MNC. Spectrochim. Acta B. 1984; 39:1567.
18. Morgan AE, Degrefte HAM, Warmoltz N, Werner HW, Tolle HJ. Appl. Surf. Sci. 1981; 7:372.
19. Reuter W. Nucl. Instrum. Meth. B. 1986; 15:173.
20. Reuter W, Wittmaack K. Appl. Surf. Sci. 1980; 5:221.
21. Alay JL, Vandervorst W. Phys. Rev. B. 1994; 50:15015.

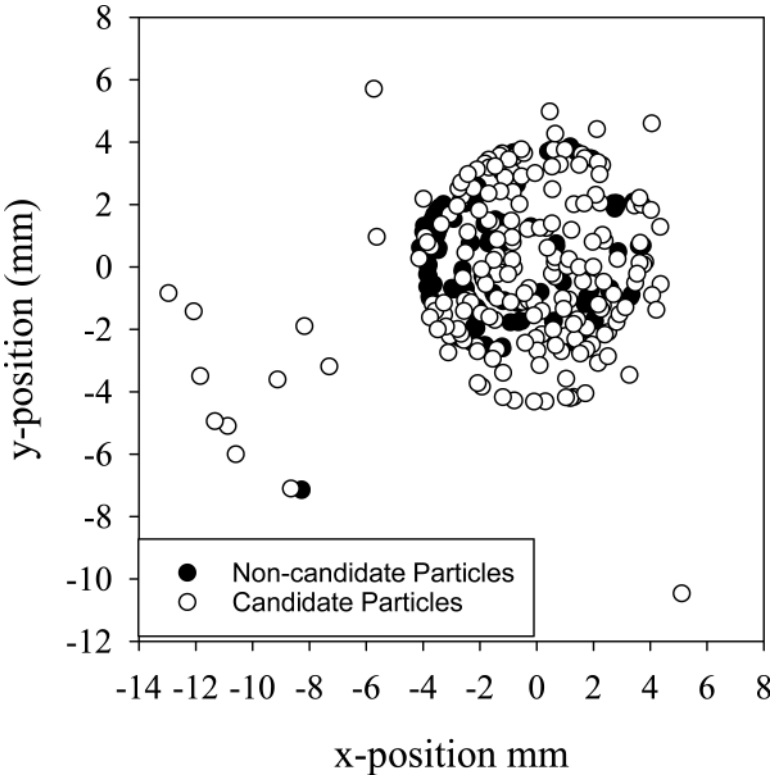

Fig. 1.

SEM/EDX map for uranium particles defined as candidates (single particles that are well separated from neighbors; open circle) and non-candidates (filled circle). Dimensions have been transformed to SIMS coordinates and are listed in millimeters (mm). Particle diameters are 1 μm and are not to scale in this figure.

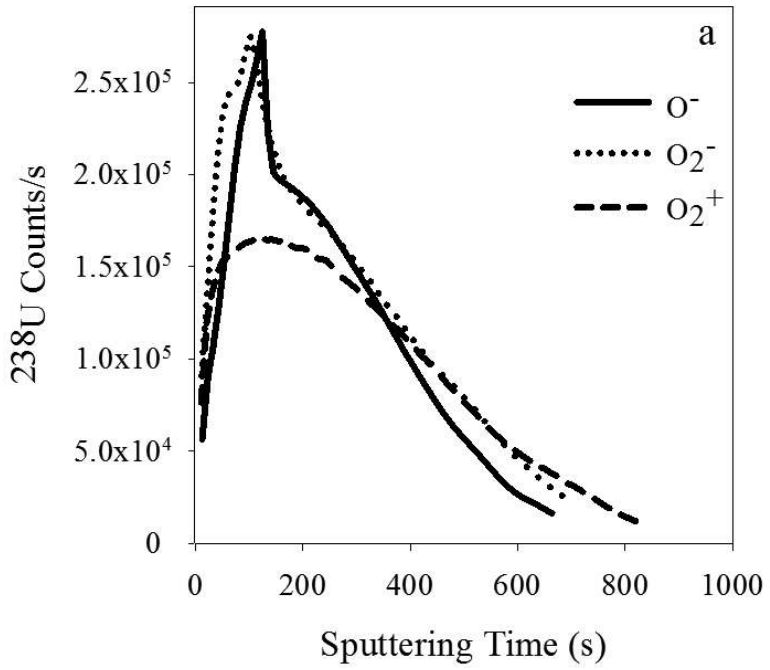

Figure 0002

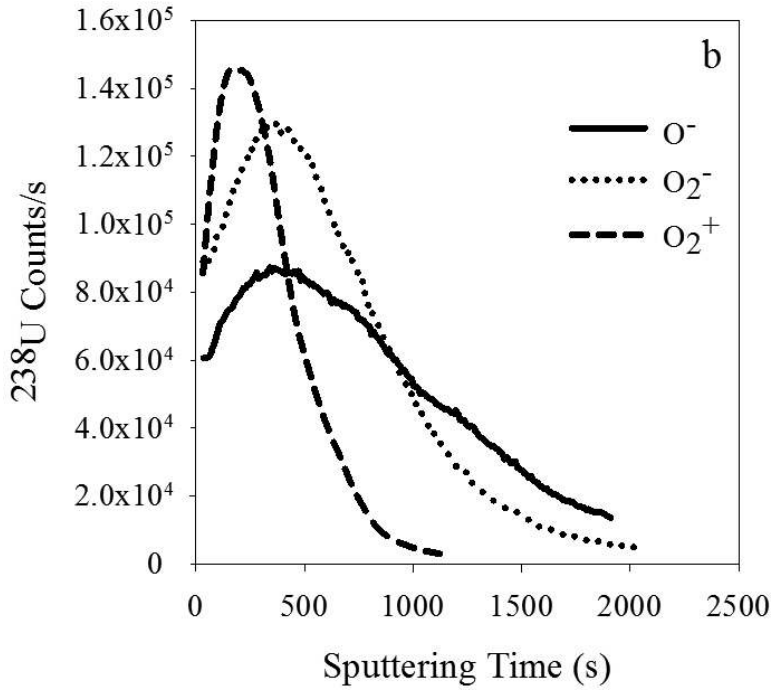

Figure 0003

Fig. 2.

Typical uranium microsphere sputter profiles for particles on silicon (a) and graphite (b). The x-axis is in seconds and the y-axis is in ^{238}U counts per second.

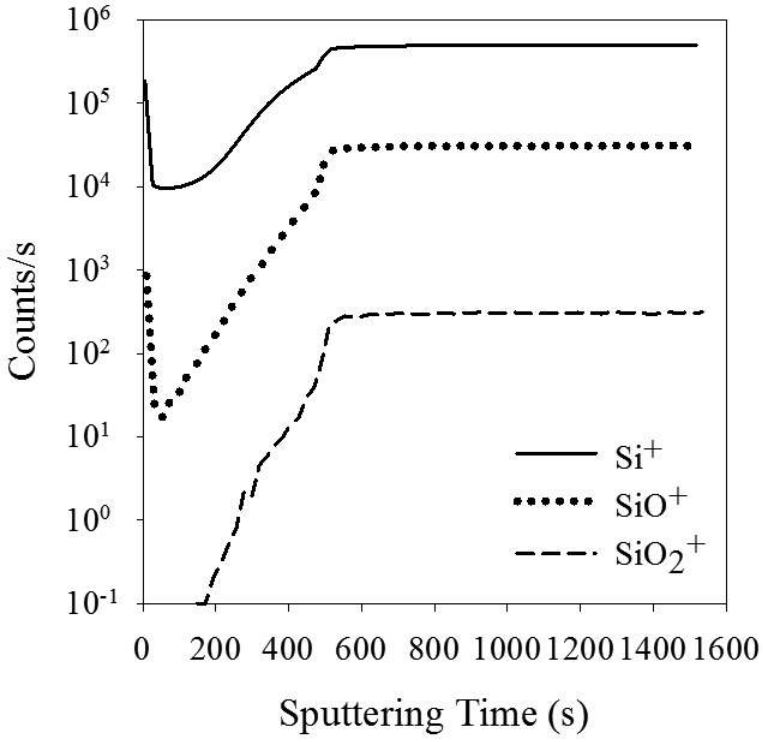

Fig. 3.

Silicon and silicon oxide ion profiles when sputtered with O^- primary ions. Similar profiles are obtained using O_2^- ion beams. The x-axis is in seconds and the y-axis is in counts per second.

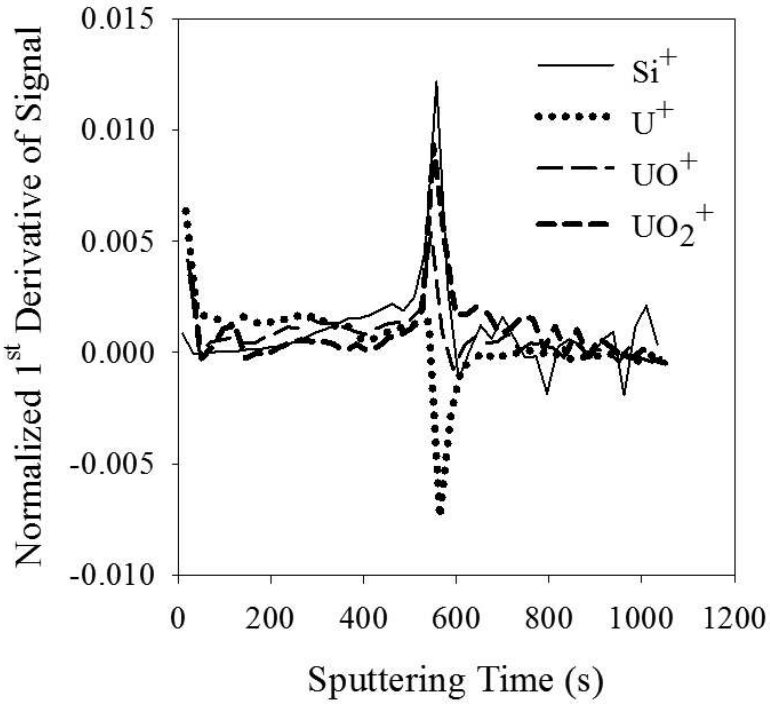

Fig. 4.

Normalized signal first derivative profiles vs sputter time in seconds from a uranium particle on silicon substrate sputtered with O^-.

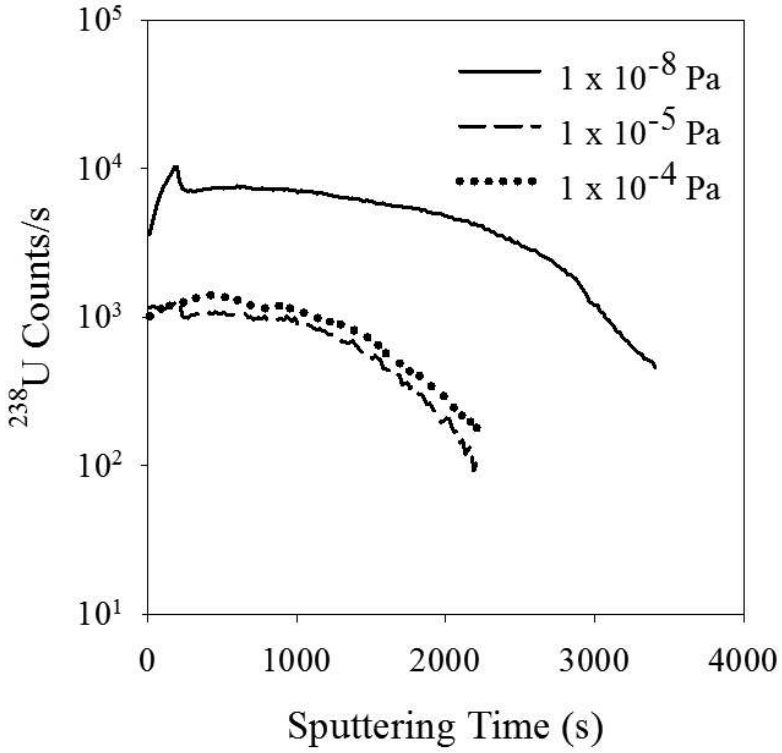

Fig. 5.

Profile of uraninite particles sputtered with O^- primary ion beam at base pressure (1×10^{-8} Pa) and increasing oxygen leaks. The x-axis is time sputtered in seconds and the y-axis is ^{238}U counts per second.

Table I

Primary and secondary ion optic parameters for silicon and carbon substrates.

Primary ions	**O^-**	**O_2^-**	**O_2^+**
Primary acceleration voltage	−13 kV	−13 kV	+15 kV
Secondary acceleration voltage	+10 kV	+10 kV	+7 kV
Impact energy	23 keV	23 keV	8 keV
Primary beam angle	22.1°	22.1°	43.2°
Contrast aperture	400 μm	400 μm	400 μm
Field aperture	8000 μm	8000 μm	8000 μm
Entrance slit	250 μm	250 μm	250 μm
Exit slit	500 μm	500 μm	500 μm
Energy bandpass	50 eV	50 eV	50 eV
Raster (Carbon planchet only)	10 μm × 10 μm	10 μm × 10 μm	10 μm × 10 μm

Table II

Total ion efficiencies for uranium particles when sputtered with O^-, O_2^-, and O_2^+ on carbon and silicon mounts including previous results from Ranebo *et al,* [2], where data from O^- comes from a Cameca IMS-6f and data from O_2^- and O_2^+ comes from an IMS-1270.

	Graphite			Silicon		
Primary Ions	O^-	O_2^-	O_2^+	O^-	O_2^-	O_2^+
Efficiency (%)	1.51	1.68	0.99	1.26	1.56	1.21
Standard uncertainty (1σ)	0.11	0.14	0.08	0.09	0.12	0.09
No. of particles	10	7	13	11	8	10
Ranebo Efficiency	1.27*	1.18	0.96			
Standard uncertainty (1σ)	0.06	0.15	0.07			
No. of particles	16	17	7			

*Data comes from IMS-6f